Journal of Power Sources 247 (2014) 235–242

Contents lists available at ScienceDirect

Journal of Power Sources

journal homepage: www.elsevier.com/locate/jpowsour

High figure of merit for electrokinetic energy conversion in Nafion membranes

Bjørn Sjøgren Kilsgaard, Sofie Haldrup, Jacopo Catalano, Anders Bentien*

Department of Engineering, Aarhus University, Langelandsgade 140, 8000 Aarhus C, Denmark

HIGHLIGHTS

- High electrokinetic energy conversion efficiency in Nafion membrane is found.
- Electrokinetic figure of merit is investigated experimentally.
- Highly charged membranes have not been considered for electrokinetic energy conversion.
- Low cost electrokinetic energy conversion may be possible.

ARTICLE INFO

Article history:
Received 24 May 2013
Received in revised form
6 August 2013
Accepted 17 August 2013
Available online 31 August 2013

Keywords:
Nafion
Electrokinetic energy conversion
Figure-of-merit
Conversion efficiency
Charged membrane

ABSTRACT

Based on measurements of the streaming potential coefficient, hydraulic permeability and ion conductivity the electrokinetic energy conversion of nanoporous ion conductive Nafion®117 polymer membrane has been evaluated. A high figure-of-merit of 1.1 ± 0.2 has been found in 0.03 M aqueous LiCl solution that corresponds to an electrokinetic energy conversion efficiency of approximately 18 ± 2%. To the best of our knowledge, this is the first study in the literature designated to the electrokinetic energy conversion in materials where the pores have high surface charge density. The initial results are promising with respect to future electrokinetic generator or pump applications and highly charged polymer membranes might be a future pathway for low-cost high-efficiency electrokinetic energy conversion.

1. Introduction

The fundamental mechanism of electrokinetic effects is the coupling of the movement of ions and a solvent. In aqueous solvents this coupling arises from the hydration effect which is caused by electrostatic interactions between the charged ions and polar water molecules. Electrokinetic effects can be utilized for direct conversion of electrochemical energy into kinetic energy or vice versa [1], i.e. in electroosmosis, water molecules are dragged along with an ionic current and functions as a pump. In the reverse operation a pressure gradient creates a flux of water that drags ions along with it inducing a streaming potential that can be utilized for power generation.

State-of-the-art with respect to commercial devices that can convert kinetic energy and electrical energy is dominated by electromagnetic actuators that are coupled to mechanical stages i.e. pumps, generators or turbines. Less used technologies are based on e.g. the piezoelectric effect [2], electro active polymers (EAP) [3] including the ones based on ion conductive membranes [4]. A unique property of electrokinetic energy conversion is the direct coupling between ions and solvent, this result in pumps and generators that does not require moving mechanical stages such as shafts, rotors, turbines, diaphragms etc. In certain applications this property can make electrokinetic devices more feasible than electromagnetic, piezoelectric or EAP based devices. If high efficient electrokinetic energy conversion devices can be realized some of the potential applications within actuation will be microfluidic pumps, compressors for cooling cycles, advanced electrodialytic separation processes (combined desalination and dewatering); recently, also as thruster for space propulsion [5] has been suggested. With respect to power generation some of the potential applications are domestic generators in (solar) heat engines e.g. organic Rankine cycles [6], compressed air energy storage [7] or a

* Corresponding author.
E-mail address: bentien@ase.au.dk (A. Bentien).

0378-7753/$ – see front matter © 2013 Elsevier B.V. All rights reserved.
http://dx.doi.org/10.1016/j.jpowsour.2013.08.067

combination of both. The feasibility of potential applications depends strongly on the parameters like energy conversion efficiency, power density and capital investment. To this end it is noted that pumps and generators can reach very high first law efficiencies above 90% as seen for large turbines/generator in hydroelectric plants or for large high pressure pumps for desalination purposes. Nonetheless, the general trend is that the efficiency decreases with power and it is typically below 50% in state-of-the-art frequency controlled pumps in the 1 kW range [8] and the target of alternative energy conversion technologies is most likely to be in this range and below.

Electrokinetic energy conversion was initially studied theoretically in the 1960's by Osterle and co-workers [1,9] and Burgreen and Nakache [10,11] that predicted maximum first law efficiencies (η_{EK}) of the order 1–3% and up to 17%, respectively. During the past decade renewed interest in this topic has emerged; most reports focus on the theoretical transport properties of straight nanochannels with well-defined dimensions [12–27]. However, only a few experimental investigations [12,28–32] have been reported in which η_{EK} up to 10% has been measured. Nonetheless, recent theoretical development has shown that η_{EK} much larger than 10% may be obtained in pores with slip flow [16,18,25] or in pores where there is a counter ion layering that displaces some of the counter ions away from the pore wall [26,27]. Both effects increase with the surface charge density (σ_0) [16,18,25,26].

Recently, the electrokinetic properties of low charged membranes with pore sizes in the range from 25 to 1000 nm were investigated, and a maximum estimated conversion efficiency of about 7% was found [32]. In the current work we present the electrokinetic properties of commercial Nafion®117 membranes, in the following referred to as Nafion. In contrast to the previous study, Nafion is a highly charged membrane with an ion exchange capacity of ~0.95 meq g^{-1} dry membrane. Assuming, as a first approximation, that the fixed charges are evenly distributed in the membrane this corresponds to a surface charge density of approximately 0.2 C m^{-2} in good agreement with other assessments of $\sigma_0 \sim$ 0.2 C m^{-2}–1 C m^{-2} in the pores of Nafion [33,34].

The detailed structure of Nafion in the swollen state has been contentious. Indeed in its solvated state Nafion presents a rather complex structure since it can be depicted as a heterogeneous medium in which a hydrophobic PFTE-like backbone phase coexists with a hydrophilic region formed by the side-chain $-SO_3H$ groups and water molecules. Different models have been proposed to describe such a two-phase structure; e.g. the standard Gierke's model [35] of network formed by spherical water cluster interconnected by narrow 1-nm channel, local-order model [36] hydrated bilayers [37,38] and network models [39] among the others. Analysis of small-angle X-ray scattering data showed that the Nafion structure could be accurately explained as parallel cylindrical nanochannels [40] with diameters ranging between 1.8 and 3.8 nm at 20 vol% water content. Despite the differences in the proposed structures, the excellent transport properties of Nafion membranes are believed to be related to the interconnected water network inside the polymer matrix, with channel dimension ranging approximately between 1 and 5 nm.

Direct measurement of the electrokinetic conversion efficiency is inherently challenging from an experimental point of view. In particular contact resistance between electrodes and membrane might diminish the measured efficiency compared to the possible maximum efficiency of the membrane. Furthermore, a direct measurement of the conversion efficiency does not reveal detailed information about the properties of the membranes. As an alternative, we use in the present study the method of measurement of the electrokinetic figure-of-merit (β_{EK}), from three independent transport coefficients. The method is fully equivalent to the measurement of the thermoelectric figure-of-merit, that is the gold standard for assessing the goodness of materials for thermoelectric energy conversion [41]. The advantage is that if proper experimental conditions are fulfilled, the assessment of the conversion efficiency is intrinsic to the material and independent of e.g. electrode contact resistance.

From the phenomenological transport equations and Onsager relations it can be shown [1,9] that the first law efficiency defined for the electrokinetic conversion, η_{EK}, increases with β_{EK} through the relation $\eta_{EK} = [(1+\beta_{EK})^{1/2} - 1]/[(1+\beta_{EK})^{1/2} + 1]$, where $\beta_{EK} = [(L_{\nu\nu}L_{\phi\phi}/L_{\nu\phi}L_{\phi\nu}) - 1]^{-1}$ and L_{ij} are phenomenological transport coefficients. β_{EK} can be evaluated by measuring transport properties that contain the cross coupling transport coefficient $L_{\nu\phi}$ e.g. electroosmotic pressure, streaming current, streaming potential coefficient etc. together with the conductivity terms $L_{\nu\nu}$ and $L_{\phi\phi}$, i.e. hydraulic permeability and ion conductivity. Using the streaming potential coefficient (ν) together with the hydraulic permeability (κ_H) and ion conductivity (σ), results in $\beta_{EK} = \nu^2 \cdot \sigma/\kappa_H$ (the reader is referred to Ref [32] for a more detailed discussion). We have chosen to evaluate β_{EK} from ν since this transport coefficient is an intensive variable that is relatively easy to correct for concentration polarization effects and is measured with good accuracy.

It is noted that in $\beta_{EK} = \nu^2 \cdot \sigma/\kappa_H$, the membrane geometry is present in both the numerator (σ) and denominator (κ_H) and cancels out leaving β_{EK} as an intensive variable. Hence errors in the measurement of the membrane geometry do not influence the evaluation of β_{EK} provided that all measurements are done in the same electrochemical cell.

To the best of our knowledge, the current work is the first designated study of electrokinetic energy conversion in highly charged ion conducting membranes in the literature. An experimental characterization of the transport properties including ion conductivity, streaming potential coefficient and hydraulic permeability of Nafion membranes in LiCl solutions is presented.

2. Experimental

A membrane sheet (30 cm × 30 cm) of Nafion 117 was bought from Ion Power Inc. The membrane potential and water uptake were measured for the general characterization of the membrane. For the determination of β_{EK} the streaming potential coefficient, ion conductivity and hydraulic permeability have been measured. These measurements were all conducted in the same electrochemical cell and with the same membrane sample. The membrane potential and water uptake have been measured on different samples from the same membrane sheet. Before use, the membrane pieces were pretreated by heating it up in demineralized water until boiling. The membrane was then transferred to a 0.05 M sulfuric acid solution at ~90 °C, where it was kept for 10 min followed by thorough washing in warm demineralized water (~70 °C). After pretreatment the membrane was stored in a 0.1 M LiCl solution until use. All measurements of the transport coefficients (ν, σ and κ_H) have been performed in 0.03 M LiCl solutions and before use the membrane was rinsed in 0.03 M LiCl to avoid an increase of the LiCl concentration in the electrochemical measurement cell.

The membrane potential was measured in a concentration cell, consisting of two identical Teflon chambers, separated by the membrane with an active area of 0.785 cm^2. In the experiments the two chambers were filled with LiCl solutions with a concentration ratio of 1:2 and magnetically stirred at 1500 rpm to minimize the effect of concentration polarization. Two salt bridges, 28 wt% KCl and 1.5% Agar (Select Agar, Sigma Aldrich), were mounted between the cells and two KCl saturated solutions in which the Ag/AgCl

electrodes (reference electrodes, Schott) were placed to measure the membrane potential.

The water uptake was determined gravimetrically comparing the Nafion sample weight before and after the polymer was soaed in 0.1 M LiCl solution for at least 24 h. It is worth to note that the dry mass of the samples was measured after a drying procedure performed in a recirculating oven at 50 °C. As known from the literature this procedure did not allow the complete removal of the H_2O absorbed by the perfluorosulfonic acid ionomeric membranes from the water moisture present in the atmosphere, due to the high interaction between the sulfonic groups and H_2O molecules [42,43]. As a consequence the measured uptake, expressed as $\lambda = n_{H_2O}/SO_3^-$ could be an underestimation of the real solubility. The membrane thickness in both the dry and swelled state was measured by means of a digital micrometer (Diesella, resolution 1 μm).

The electrodes used for measuring ν and σ were made from ≥99.99% Ag wire with 0.25 mm diameter purchased from Sigma Aldrich using a procedure adopted from Ref. [44]. The Ag/AgCl electrodes were prepared by polishing the as-received silver wire with fine sandpaper to remove impurities. The Ag wire was then dipped in concentrated nitric acid (∼68%) for 10 s then immediately dried. After the cleaning procedure, the Ag wire was electroplated in a 0.05 M KCl solution with a current density of 1 mA cm^{-2} for approximately 25 min, which resulted in electrodes containing about 2.5 mol% AgCl. After electroplating the electrodes were stored in a 0.03 M LiCl solution for at least 24 h in a dark and oxygen-free environment. All solutions used for making the electrodes were purged with argon before use.

The electrochemical cell for the measurement of ν, σ and κ_H is schematically shown in Fig. 1. For the streaming potential and hydraulic permeability measurements Series-96705 pressure sensors (0–20 bar) from AB Elektronik Sachsen GmbH were connected through the ports 7 and 8, pressure was generated through port 6 with pressurized argon gas and the solute flux through the membrane exits the cell through port 1. Ag/AgCl electrodes were inserted through port 2 and 5 and connected to a National Instruments NI-9219 card (NI-9219). Fine grid stainless steel support material on the low-pressure side prevents the membrane from deformation while under stress due to the applied pressure difference. If a fine grid support coated with PTFE is used, it becomes too hydrophobic and very difficult to wet, hence altering the experimental results. In any case, the potential difference across the support is so low that no electrochemical reactions are induced. In this setup the active membrane surface area is 2.54 cm^2.

The instrumentation for the measurement of hydraulic permeability was the same as for the streaming potential; in this case the volume flow through the membrane was measured from the movement of the meniscus in a capillary with an inner diameter of 0.75 mm mounted in port 1.

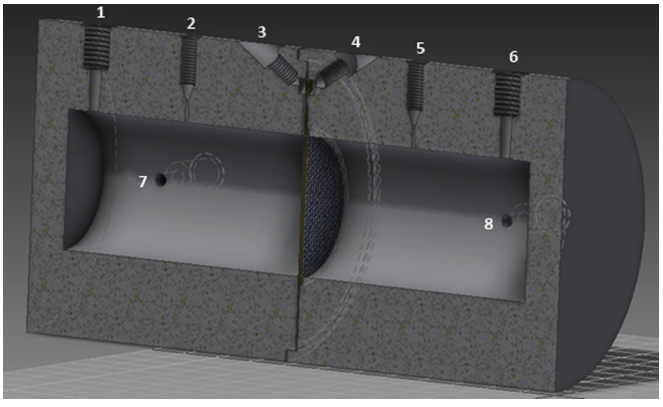

Fig. 1. Drawing of the electrochemical cell used for the measurement of ν, σ and κ_H. The active area of the membrane is 2.54 cm^2.

The ion conductivity was measured with a four-point probe method. Ion current was generated with Ag/AgCl electrodes connected through port 2 and 5 with an Agilent U2722A Source Measure Unit. The potential difference was measured with Ag/AgCl electrodes connected through port 3 and 4 with an NI-9219 card. The electrodes are located in small chambers with approximate size 2 × 2 × 2 mm connected by narrow channels (0.5 mm width and 0.5 mm depth) to the large main compartments. The small chambers and channels are in direct contact with each side of the membrane surface. This setup is similar to a four-point probe with Haber–Luggin capillaries, however, with the current setup it is possible to measure the potential difference very close to the surface of the membrane, hence the potential drop due to solution resistivity is minimized and no correction has been applied. During the ion conductivity measurements the membrane support was removed.

Unless otherwise stated all measurements were performed with stirring in order to minimize concentration polarization effects. All data, except volume flow, has been recorded continuously with Labview SignalExpress at 1.95 Hz and at room temperature (22 °C ± 1 °C).

3. Results

3.1. Membrane potential and water uptake

The dry membrane had a thickness (Δx) of ∼183 μm while in the 0.03 M LiCl solution Δx was approximately 201 μm. This latter value was used in the calculation of the extensive transport parameters σ and κ_H.

The water uptake was found to be 0.33 g water/dry membrane corresponding to $\lambda = 20.1$ water molecules per SO_3^- group, taken as an average of 4 different measurements: this value is in good agreement with $\lambda = 20.0 \pm 0.3$, 22.3 and 18.2 found for thermally pretreated Nafion membranes in Li^+ form by Evans et al. (Nafion 117) [45], Steck and Yeager (Nafion 120) [46] and Gierke and Hsu (Nafion 120) [47], respectively. However, there is a certain degree of uncertainty associated with the water uptake in Nafion membranes in Li^+ form since in the literature are reported values of $\lambda = 16.5$ (Nafion 117) [48] and 24.2 (Nafion 115) [49].

The membrane potential was measured in solutions with concentration of 0.01/0.02 M, 0.1/0.2 M and 1.0/2.0 M LiCl. Nafion showed membrane potentials close to the theoretical limit for the two most dilute solutions (16.3 and 16.4 mV for 0.01/0.02 and 0.1/0.2 M LiCl respectively) while a slight decrease with respect to theoretical limit was observed for 1.0/2.0 M solution (12.3 mV). The membrane potentials were converted into cation transport numbers [50] and the theoretical upper limit values calculated by using the activity coefficients found in Ref. [51]. In the presence of dilute solutions the calculated transport numbers were 0.98 and 0.99 resulting in a high permselectivity of the Nafion membrane.

3.2. Hydraulic permeability

Fig. 2 shows the data for the determination of the hydraulic permeability of the Nafion membrane. The upper panel of Fig. 2 shows the volume (V/A) conducted through the membrane per unit of membrane surface area as function of time. To investigate the effect of concentration polarization a few measurements without stirring in the cell are also included in the plot. In all experiments V/A had a non-linear time dependence for $t \lesssim 300$–600 s and to the limit of the resolution of the data $V/A(t)$ becomes

linear for larger times. Similar observations are reported in literature [52,53].

The major part of the non-linear effect is non-intrinsic and related to mechanical movement of membrane and membrane holder whenever the pressure was applied. This stabilizes on a timescale of the order a few seconds. Still, after this stabilization there is a non-linear effect that continues up $t \lesssim 300–600$ s. The effect is relatively larger for low pressures. It could be related to concentration polarization effects, but additional data (not shown) indicates that the effect is independent of stirring. Alternatively, it is our hypothesis that this could be related to some mechanical relaxation or strain of the membrane whenever pressure is applied, with a timescale of the order of a few minutes. The effect has also been observed in the streaming potential measurements as shown later.

The volume flux (j_v) are determined from linear fits of $V/A(t)$ in the linear region and are shown, as function of pressure difference across the membrane (Δp), in the lower panel of Fig. 2. The hydraulic permeability is determined from linear fits between j_v and Δp constrained to pass through the origin and normalized with

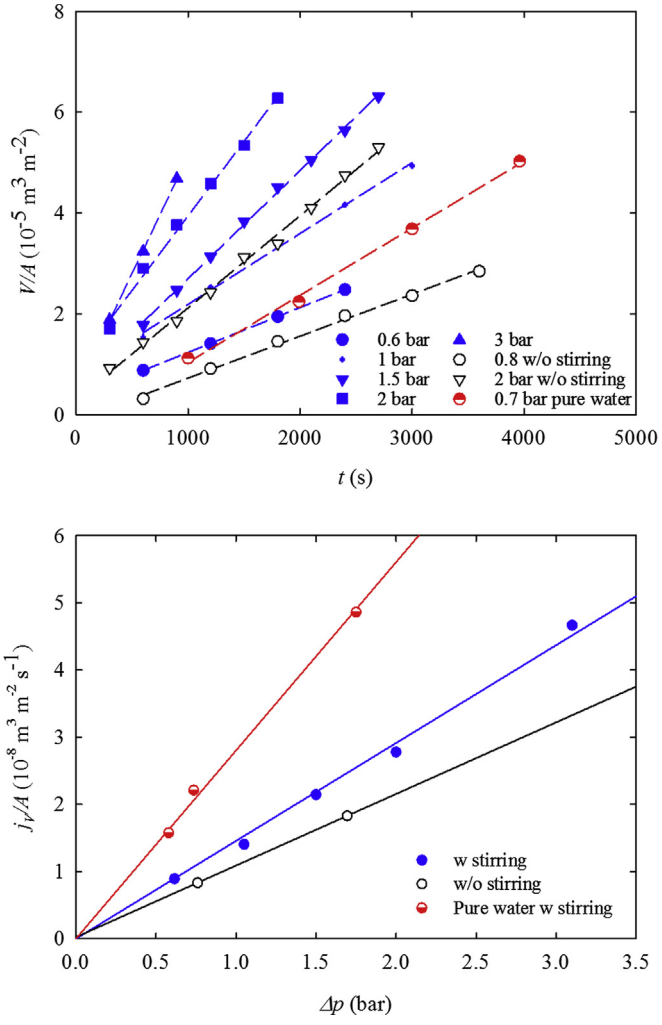

Fig. 2. The upper panel shows the total volume conducted through the membrane per unit area as function of time (t) at different pressure differences (Δp). Straight lines are linear fits of data in the linear region where the slopes define the volume flux per unit area. The lower panel shows the volume flux as function of pressure difference (Δp). The hollow and solid data points are recorded without and with stirring in the cell, respectively. The straight lines are linear fits to the data points constrained to pass through the origin.

respect to the membrane thickness. Three different experimental conditions were tested; (i) with stirring, (ii) without stirring for the membrane in 0.03 M LiCl and (iii) with stirring in pure water using a membrane in H^+ form (iii). The corresponding experimental hydraulic permeabilities were $\kappa_H = 3.1 \cdot 10^{-17}$, $2.1 \cdot 10^{-17}$ and $5.6 \cdot 10^{-17}$ m^2 Pa^{-1} s^{-1}, respectively.

As expected the highest κ_H is found in pure water with a membrane in H^+ form. Here concentration polarization effects are absent and the electroviscous/dragging effects are diminished since the water transport number of H^+ is almost an order of magnitude lower than that of Li^+ [54]. At the same time the water uptake of Nafion on the H^+ and Li^+ are very similar [45], which means that the pore size is unaltered in the two forms. In further agreement with expectations the lowest κ_H is observed in the experiment (ii) without stirring where concentration polarization effects contributes to the hydraulic resistance.

κ_H has also been determined on different Nafion membrane samples (data not shown), different electrolyte solutions (e.g. NaCl) and also on a different experimental setup than the one used in the present study. In all measurements of κ_H were in the same range as the above values ($2.1 \cdot 10^{-17}$ m^2 Pa^{-1} s^{-1}–$5.6 \cdot 10^{-17}$ m^2 Pa^{-1} s^{-1}).

Values of κ_H for Nafion 117 in the literature [45,52,53] varies up to two orders of magnitude from approximately $0.2 \cdot 10^{-17}$ m^2 Pa^{-1} s^{-1} to $20 \cdot 10^{-17}$ m^2 Pa^{-1} s^{-1} and even larger if Nafion 117 membranes without pretreatment are included in the comparison [45]. This variation is much larger than what can be expected from electroviscous effects and different electrolyte solutions. Evans et al. showed [45] that heat and chemical pretreatment of Nafion membranes affect κ_H by up to an order of magnitude and that κ_H increased with the water content. Still, this phenomenon cannot explain the different values reported in the literature, and we note that κ_H systematically decreases with the applied pressure, i.e. the measurements of Villaluenga et al. [52,53] and Evans et al. [45] were performed in the range 0.3–0.8 bar and 50–150 bar, respectively, while the measurements reported in the present work are performed in the range in the range 0.6–3.0 bar. This variation with pressure could possibly be related to differences in mechanical relaxation or strain of the membrane whenever pressure is applied, however, a systematic study of these phenomena is outside the scope of the present work. In any case and irrespective of the mechanism behind the differences we are confident with respect to the accuracy of κ_H in our measurements.

3.3. Streaming potential

Initially the stability of the electrodes in the measurement cell was determined. As an example Fig. 3 shows the potential (ϕ) as function of time in the measurement cell with a membrane inserted without pressure applied. It is seen that the electrodes are very stable over several hours and the drift rate is less than 5 μV h^{-1}.

The streaming potentials have been determined experimentally by two different methods. In the first, stirring has been applied to the cell during the measurement in order to minimize the effects of concentration polarization phenomenon. An example of these experiments is shown in Fig. 4, that plots the potential (ϕ) as function of time with a trans-membrane pressure difference of 0.6 bar. After a sharp increase when pressure is applied, ϕ decreases slowly with time reaching a constant value after approximately 600 s. We anticipate this decrease to be related to the nonlinear volume flow for $t \lesssim 300–600$ as discussed in the previous section. However, due to the slow data sampling rate in the hydraulic permeability measurements it is not possible to make definite experimental proof of this. A similar effect was observed when the pressure difference across the membrane was removed, here the stabilization of ϕ occurs on the timescale 500–1500 s. Since the electrodes in the

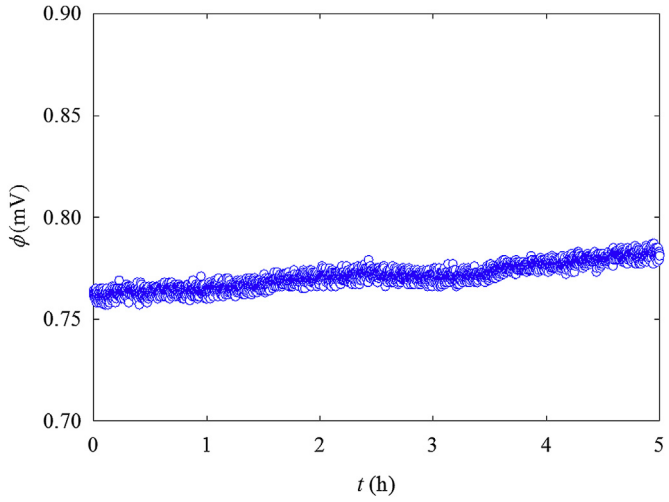

Fig. 3. Example of the electrode stability in the measurement cell. The plot shows the potential (ϕ) as function of time (t), that drift less than 5 μV h^{-1}.

measurement cell drift less than 5 μV h^{-1}, when it is left undisturbed for many hours, we suggest that this is due to mechanical relaxation effects of the membrane back to the state where no stress is applied.

As mentioned earlier this effect was relatively smaller when pressure was increased. For measurements conducted at ≥1.5 bar the effect was much less pronounced and ϕ stabilized faster with time. This is indicated in Fig. 5 which shows a measurement with a 3 bar trans-membrane pressure difference. When stirring is turned on after 200 s, ϕ stabilized within 60 s, meaning that no relaxation effects are observed (at least after 260 s).

In any case the streaming potential was determined from values of ϕ after it has stabilized as indicated by ϕ_H and ϕ_L used for determination of $\Delta\phi = \phi_H - \phi_L$ in Fig. 4.

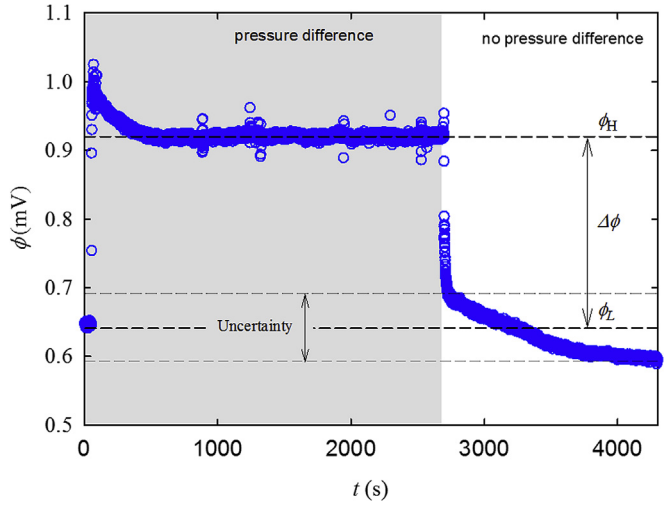

Fig. 4. Example of streaming potential measurement with stirring in the cell. At $t = 0$ s a pressure difference of 0.61 bar was applied. The potential (ϕ) increases to about 1 mV in a few seconds and decreases slowly within approximately 600 s to a constant value of about 0.92 mV. At $t \sim 2700$ s the pressure difference across the membrane is removed and ϕ decreases rapidly within a few seconds to a value of 0.69 mV followed by a slowly decrease to a constant value of approximately 0.59 mV. The potential difference ($\Delta\phi$) between the high (ϕ_H) and low (ϕ_L) values are used for calculating the streaming potential coefficient $\nu = \Delta\phi/\Delta p$. The relatively large noise ($\phi_{RMS} \sim 10$ μV) is generated by the electromagnetic stirrers.

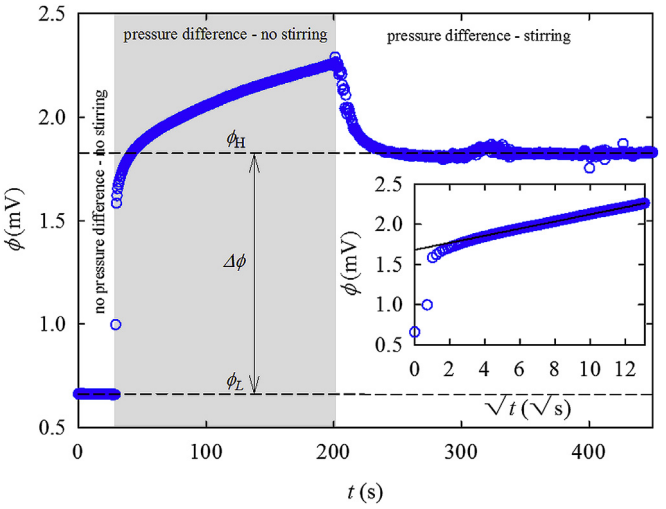

Fig. 5. Example of streaming potential measurement initially without stirring and stirring turned on at $t \sim 200$ s. At $t \sim 30$ s a trans-membrane pressure difference of 3.0 bar is applied. The potential (ϕ) increases rapidly to a value of approximately 1.6 mV in about a second, followed by a slower increase with time. At $t \sim 200$ s the stirring is turned on and ϕ decreases rapidly to a constant value of approximately 1.8 mV. The difference ($\Delta\phi$) between the high (ϕ_H) and low (ϕ_L) values are used for calculating the streaming potential coefficient $\nu = \Delta\phi/\Delta p$ when the concentration polarization layer is diminished. The inset shows the same data but as function of $\sqrt{t}$ up to $t \sim 200$ s, where stirring is applied. The RMS value of the noise level when stirring is turned off is approximately $\phi_{RMS} \sim 1$ μV.

The second method for the determination of the streaming potential has been developed and theoretically described by Okada et al. [55]. In this method the streaming potential is measured with no stirring and an undisturbed concentration polarization layer is allowed to build up. The transport of ions in and out of the boundary layer is in this case due to diffusion only, and the time dependence of the streaming potential can be described by: $\Delta\phi(t) = \nu\Delta p + A\sqrt{t}$, in which the $\sqrt{t}$ increase, is the characteristic time-dependence for diffusion-limited processes. The constant A is dependent on the hydraulic permeability, diffusion coefficient of the salt and transport numbers of the ions in solution and membrane [55]. In the present study we use the time dependence to extrapolate $\phi(t)$ to $t = 0$ where the concentration polarization layer is not built up, hence the streaming potential without concentration polarization can be determined.

Fig. 5 shows an example of a measurement of $\phi(t)$ in the cell without initial stirring. When the pressure difference $\Delta p = 3.0$ bar is applied $\phi(t)$ increases rapidly followed by a slower increase. The inset shows the same data but only in the time span where no stirring is present and as function of $\sqrt{t}$. A linear relation is seen and ϕ can be extrapolated to $t = 0$ where $\phi H = 1681$ μV. Combined with the $\phi_L = 660$ μV, $\Delta\phi = \phi_H - \phi_L$ is determined to 1021 μV for the measurement without stirring.

In order to test if a measurement with stirring reproduces this streaming potential, stirring is applied after approximately 200 s and $\phi(t)$ decreases to a constant value after approximately 60 s. Again with reference to Fig. 5 it is seen that $\phi(t)$ reaches a constant value (ϕH) of 1820 μV after approximately 60 s resulting in $\Delta\phi = 1160$ μV. In this specific measurement the two values of $\Delta\phi$ obtained by two different methods vary approximately 12%.

In Fig. 6 all streaming potential measurements are plotted as $\Delta\phi$ versus Δp. For both the direct measurement of the streaming potential (with stirring) and the indirect (without stirring) a good linear relationship is seen at higher pressures. At lower pressures $\Delta\phi$ varies systematically from the linear relationship and it is suggested that this deviation is either directly related to mechanical

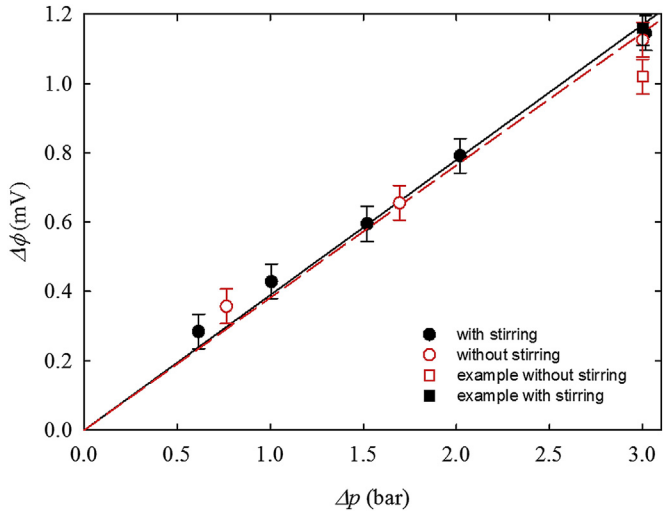

Fig. 6. Potential differences ($\Delta\phi$) from streaming potential measurements as function of pressure differences (Δp). Examples of how $\Delta\phi$ is found experimentally is shown in Figs. 4 and 5. The two data points denoted as examples are the ones from Fig. 5 and are included for completeness. The other the data points were recorded in a separate measurement and used for the determination of the streaming potential coefficient. Straight lines are linear fits, constrained to pass through the origin, to obtain the streaming potential coefficient $\nu = \Delta\phi/\Delta p$. The potential difference ($\Delta\phi$) between the high (ϕ_H) and low (ϕ_L) values are used for calculating the streaming potential.

relaxation effects of the membrane or due to systematic measurement errors because of this effect.

In any case the streaming potential coefficient is determined from a linear fit constrained to pass through the origin and to data points in the linear region above 1.5 bar and find $\nu = 390$ μV bar^{-1} and 382 μV bar^{-1} for the measurements with and without stirring, respectively.

To the best of our knowledge, only one work [56] on the streaming potential of Nafion 117 membranes in (0.03 M) LiCl solutions has been reported in literature. In Ref. [56] ν is reported in terms of the water transport number (t_w) which corresponds to ν approximately 295 μV bar^{-1}. Furthermore, electroosmosis measurements [57] on Nafion 117 membranes in 0.01 M LiCl results in $\nu \sim 245$ μV bar^{-1} assuming that the Saxén relation between electroosmosis and streaming potential holds. All three values are of similar magnitude and we attribute the differences to be a combination of membrane-batch dependence and differences in the pretreatment of the membranes.

3.4. Ion conductivity

Fig. 7 shows the experimental results for the determination of the ion conductivity of the Nafion membrane. The upper panel is an example of raw data from a measurement where a current (I) is passed through the membrane while the potential (ϕ) difference between the two electrodes on each side of the membrane is measured. When the current is applied it reaches a steady state value within milliseconds. The corresponding potential difference between the two electrodes goes from a low offset value (ϕ_L), of the order 20 μV–100 μV, up to a high value (ϕH) in milliseconds and on the same timescale as the current. This is followed by a slower increase with time and we associate the potential difference $\Delta\phi = \phi H - \phi_L$ with the intrinsic membrane resistance and a small contribution from the electrolyte solution in the near vicinity of the surface. The slow increase is attributed to concentration polarization effects.

The lower panel of Fig. 7 shows $\Delta\phi$ as function of I. From a linear fit constrained to pass through the origin a resistance of 0.33 Ω is

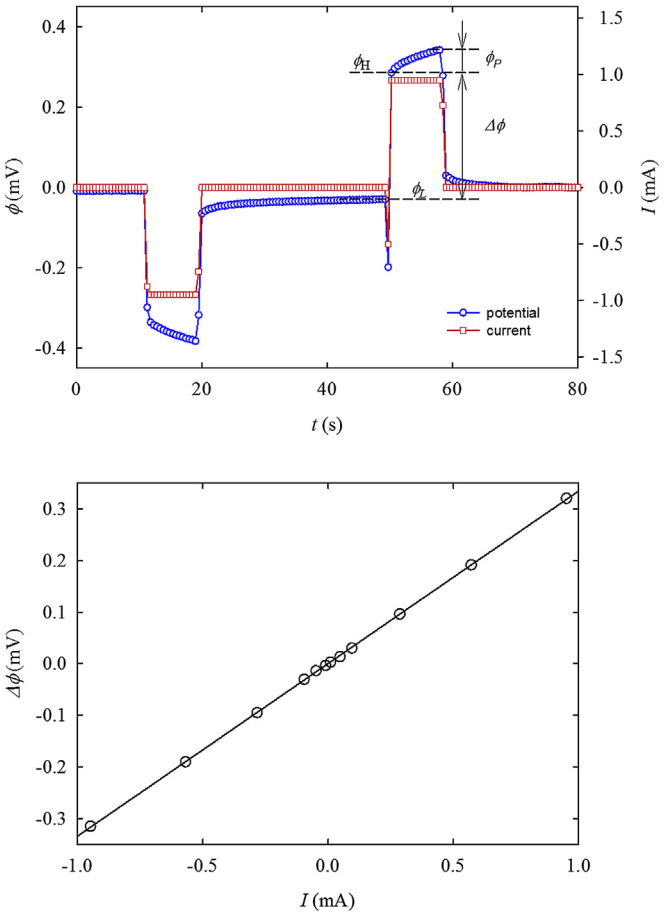

Fig. 7. Upper panel: example of the potential difference ($\Delta\phi$) between the high (ϕH) and low (ϕ_L) generated when an ion current is passed through the membrane. ϕ_P is the effect of concentration polarization. Lower panel: potential differences ($\Delta\phi$) from conductivity measurements as function of current (I). The straight line is a linear fit, constrained to pass through the origin.

found and corresponds to a membrane ion conductivity of 2.36 S m^{-1}.

This value is in good agreement with literature values of σ measured in LiCl solutions that are approximately 3 S m^{-1} [54] and 1.61 S m^{-1} [58]. In three other studies somewhat lower values have been found 1.25 S m^{-1} [59], 0.75 S m^{-1} [48] and 0.6 S m^{-1} [4]. However, in the first two works the relatively low water uptake could explain the lower σ; $\lambda \sim 9$–11 [59] and $\lambda = 16.5$ [48], respectively. This should be compared to approximately $\lambda = 20$ found by Evans et al. for heat pretreated membranes [45] and $\lambda = 20.1$ for the membrane in the present study. In the third work [4], the membrane is presumably not heat- or pre-treated since no information about conditioning is mentioned by the authors. Standardized pretreatment is necessary in order to obtain high and reproducible ion conductivity measurement [58], and the reason for the relatively lower conductivity is most probably related to the lower water content and differences in membrane conditioning.

4. Discussion

The main objective of the current study is the estimation of the electrokinetic energy conversion efficiency in Nafion membranes. The operating conditions during energy conversion depend strongly on the mechanical setup of a specific energy conversion device. In general it can, however, be arranged in a stack with

anion/cation cell pairs similar to that of electrodialysis or a heat energy conversion devices [60], here the resistivity of the electrolyte solution in the spacing between the membranes must be included in calculations of the efficiency, this can however, be reduced by strong electrolyte solutions and short spacing between membranes compared to the membrane thickness.

Alternatively, an electrokinetic energy conversion device can be arranged with a single membrane with electrodes on the surface on each side of the membrane. Here only a cation or an anion conductive membrane is required. During operation in both arrangements there will be some level of concentration polarization at the membrane surface. This can be partially diminished with convection/stirring. Thus, even if the intrinsic membrane transport properties can be measured and the figure-of-merit/conversion efficiency calculated, the actual efficiency will depend on the operating conditions and the degree of concentration polarization.

In the following an estimate of the electrokinetic figure-of-merit ($\beta_{EK} = \nu^2 \cdot \sigma / \kappa_H$) and energy conversion efficiency is made. Table 1 summarizes all of the measured transport properties of Nafion at 0.03 M LiCl measured in the different experiments. With respect to energy conversion the most realistic operating conditions are the ones in which stirring is applied. Both the hydraulic permeability and streaming potential coefficient have been determined with stirring and are reported in Table 1 without parenthesis.

With respect to the ion conductivity the experimental setup is not suitable for measuring the effects of stirring on the potential difference across the membrane (ϕ_P) due to concentration polarization. However, it has been shown [61] that ϕ_P below the limiting current density in the steady state is proportional to the thickness of the polarization layer (t_p). Stirring effectively reduces t_p as seen from e.g. the streaming potential measurements (Fig. 5). Experimental data show [62] that t_p is reduced a factor of approximately five when stirring is applied. If it is assumed to be the case here too ϕ_P will be reduced accordingly. For the measurement with $I = 1$ mA ϕ_P will only be a fraction of $\Delta\phi \sim 300$ μV which is used in the calculation of the membrane resistance. Thus, concentration polarization in a setup with stirring will decrease the total ion conductivity of the membrane and polarization layers approximately 5–10% compared to the intrinsic ion conductivity of the membrane.

Table 1
Summary of the measured transport coefficients of Nafion in 0.03 M LiCl. The electrokinetic figure of merit (β_{EK}) is estimated from the values of the hydraulic permeability (κ_H), streaming potential coefficient (ν) and ion conductivity (σ) that are outside the parenthesis.

Transport coefficient	Value	Comment
κ_H ($m^2\ s^{-1}\ Pa^{-1}$)	$3.1 \cdot 10^{-17}$	Concentration polarization diminished (stirring)
	$(2.1 \cdot 10^{-17})$	With undisturbed concentration polarization (no stirring)
	$(5.6 \cdot 10^{-17})$	Pure water H^+ form, no electrolyte (stirring)
ν (μV bar^{-1})	390	Concentration polarization diminished (stirring)
	(382)	Intrinsic
σ (S m^{-1})	2.36	Intrinsic at $t = 0$
β_{EK}	1.2 ± 0.2	17.5% estimated experimental error (based on propagation of experimental errors of κ_H, ν and σ estimated to be 7.5%, 7.5% and 5%, respectively).
	1.1 ± 0.2	The first value is based on the intrinsic $\sigma = 2.36$ S m^{-1}, the second value is based on estimated $\sigma = 2.15$ S m^{-1} that includes concentration polarization
η_{EK} (%)	20 ± 2	Based on the intrinsic $\sigma = 2.36$ S m^{-1}
	18 ± 2	Based on estimated $\sigma = 2.15$ S m^{-1} that includes concentration polarization

Another issue that needs to be considered is the effect of the concentration polarization due to a pressure gradient on the ion conductivity. Concentration polarization effects due to an ion current and a volume flux are phenomenologically equivalent and only depend on the average salt/ion velocity relative to the solvent. The average ion velocity/drift velocity (v_d) during an electrical conductivity measurement can be found from ($j = v_d \cdot \rho \cdot n$), where j is the current density, $n \sim 0.4$ is the porosity estimated from the water uptake and $\rho \sim 9.6 \cdot 10^7$ C m^{-3} is the volumetric charge density and is determined from the ion exchange capacity assuming that the cation transport number is unity, which is experimentally verified by the membrane potential measurement. For the ion conductivity measurement with an applied current of 1 mA $v_d = 8.3 \cdot 10^{-8}$ m s^{-1} for Li^+ is found.

The average velocity of the solvent (v_s) through the membrane is the volume flux (j_v) divided by the porosity of the membrane and find $v_s = 7.8 \cdot 10^{-8}$ m s^{-1} for a trans-membrane pressure of 2 bar. This value is approximately the same as v_d, meaning that the average solvent (water) velocity is the same as average ion velocity in the two different experiments. Thus, the concentration polarization measured during ion conductivity measurements are approximately the same as it would be under electrokinetic energy conversion conditions with a pressure difference.

Using the intrinsic value of σ together with the values of ν and κ_H, $\beta_{EK} = 1.2$ is found, we estimate the experimental uncertainty of β_{EK} to be 17.5% (see Table 1 for more details). This corresponds to $\eta_{EK} = 20\% \pm 2\%$. Still if a more conservative value of σ that includes estimated concentration polarization during operation is used (2.15 S m^{-1}) $\beta_{EK} = 1.1$ and corresponds to $\eta_{EK} = 18\% \pm 2\%$. Thus, the η_{EK} found for Nafion in the present study is significantly larger than any experimental results on electrokinetic energy conversion efficiency in nano-pores and uncharged membranes reported [12,28–32]. We anticipate this value of η_{EK} to be realistic and can be obtained experimentally in a generator where a Nafion membrane is in close contact with reversible electrodes on each side.

Power densities (P/A) for electrokinetic energy conversion may be approximated from the work produced per unit time and per unit area by the liquid in the membrane, $P/A = \kappa_H / t_m \cdot \Delta p^2$. Using $\kappa_H = 3.1 \cdot 10^{-17}$ $m^2\ s^{-1}\ Pa^{-1}$ and $t_m \sim 200$ μm for a swollen Nafion membrane and assuming a pressure difference $\Delta p = 10$ bar gives $P/A \sim 1.6 \cdot 10^{-5}$ W cm^{-2} that is converted to $P/A \sim 0.31 \cdot 10^{-5}$ W cm^{-2} electrical energy using $\eta_{EK} \sim 20\%$. This is a very low value when compared to e.g. fuel cells [63] or the power density of electrokinetic energy conversion in 50 nm Nucleopore membranes where it is of the order $P/A \sim 0.091$ W cm^{-2} at 10 bar and with a 6 μm thick membrane [32]. Obviously, the power density can be significantly improved by increasing the trans-membrane pressure difference as well as using thinner membranes, but the very low hydraulic permeability of Nafion makes power densities comparable to that of fuel cells speculative.

It is emphasized that the measured figure-of-merit is obtained up to 3 bar pressure difference and extrapolation to high pressures requires that the transport properties are linear functions of the pressure. As noted earlier, the analysis of experimental literature data of κ_H for Nafion [45,52,53] indicates that this is not the case. Furthermore, the effects of concentration polarization on the streaming potential will become more significant with increasing pressures as seen by the measurement of the filtration potential [64,65]. In the present article the electrokinetic energy conversion properties have been evaluated when concentration polarization effects are diminished. The combined effect of concentration polarization at higher pressures or in the limit of no stirring on β_{EK} is at the present state unclear. In the limit of no stirring the streaming potential increases and the hydraulic permeability and the conductivity decreases, however, the combined effect on β_{EK} is

unpredictable and direct experimental determination of the conversion efficiency is required for a better understanding of the processes.

With respect to further enhancement of the electrokinetic energy conversion efficiency in aqueous electrolytes it is not expected that it can be significantly improved with any of the monovalent alkali metals. Indeed, the streaming potential coefficient generally increases with increasing hydration radius of the ion ($Li^+ > Na^+ > K^+$) [54], here H^+ is an exception due to the extra tunneling transport mechanism that reduces the water transport number and streaming potential. With respect to optimization of LiCl concentration is it also not likely that it can be improved further. The maximum β_{EK} for conventional models is normally found [12–15,19–25] for $\kappa_D \cdot d_p \sim 1$–2, where κ_D is the inverse Debye length and d_p is the pore diameter. Assuming $d_p = 4$ nm along with the LiCl concentration of 0.03 M results in $\kappa_D \cdot d_p \sim 2$ showing that further optimization with respect to concentration is also unlikely.

Using the conservative value $\eta_{EK} = 18\% \pm 2\%$ is larger than what is normally obtained by conventional theoretical models where η_{EK} up to approximately 10% is found [12–15,19–25]. Recently, however, models that include slip flow [16,18,25] or in pores where ion layering due to sterical restrictions occur [26,27] have resulted in much larger theoretical efficiencies. In both cases the effects increase with the surface charge density [16,18,25–27].

The present study is the first, for the best of our knowledge, that specifically considers electrokinetic energy conversion in a system in which pores are highly charged ($\sigma_0 \sim 0.2$ C m^{-2}–1 C m^{-2}), it is however unclear if the enhanced energy conversion efficiency is a result of slip flow and/or ion layering. In both models only relatively large pore diameters are considered while in Nafion the pore diameter is in the range 1–5 nm. In such narrow pores, flow profiles and ion layering is not well defined since the narrowest channels only are approximately 3–4 water molecules wide.

5. Summary

To the best of our knowledge this is the first designated study of the electrokinetic energy conversion efficiency of highly charged membranes in general and particularly of Nafion 117 membranes. Three independent transport coefficients, namely hydraulic permeability, streaming potential and ion conductivity have been measured in 0.03 M LiCl solutions and at room temperature. A surprisingly high electrokinetic figure-of-merit of 1.1 ± 0.2 is found and correspond to a first law energy conversion efficiency of $18\% \pm 2\%$ in experimental conditions similar to what can be expected in electrokinetic energy conversion devices. The high η_{EK} is very promising with respect to future applications of electrokinetic energy conversion in charged membranes, and shows that charged membranes may be the key for reaching even higher conversion efficiencies.

Acknowledgments

The authors gratefully acknowledge the financial support of the Villum Foundation through the Young Investigator Programme and Aarhus University Research Foundation through AU Ideas Programme.

References

[1] F.A. Morrison, J.F. Osterle, J. Chem. Phys. 43 (1965) 2111.
[2] D.J. Laser, J.G. Santiago, J. Micromech. Microeng. 14 (2004) R35.
[3] P. Brochu, Q.B. Pei, Macromol. Rapid Commun. 31 (2010) 10.
[4] K. Asaka, N. Fujiwara, K. Oguro, K. Onishi, S. Sewa, J. Electroanal. Chem. 505 (2001) 24.
[5] F.J. Diez, G. Hernaiz, J.J. Miranda, M. Sureda, Acta Astronaut. 83 (2013) 97.
[6] B. Saleh, G. Koglbauer, M. Wendland, J. Fischer, Energy 32 (2007) 1210.
[7] H.S. Chen, T.N. Cong, W. Yang, C.Q. Tan, Y.L. Li, Y.L. Ding, Prog. Nat. Sci. 19 (2009) 291.
[8] See e.g., efficiencies of a range of pumps at Grundfos Webcaps, http://net.grundfos.com/Appl/WebCAPS/custom?userid=GMAinternal.
[9] R.J. Gross, J.F. Osterle, J. Chem. Phys. 49 (1968) 228.
[10] D. Burgreen, F.R. Nakache, J. Phys. Chem. 68 (1964) 1084.
[11] D. Burgreen, F.R. Nakache, J. Appl. Mech. 32 (1965) 675.
[12] J. Yang, F.Z. Lu, L.W. Kostiuk, D.Y. Kwok, J. Micromech. Microeng. 13 (2003) 963.
[13] H. Daiguji, P.D. Yang, A.J. Szeri, A. Majumdar, Nano Lett. 4 (2004) 2315.
[14] F.H.J. van der Heyden, D.J. Bonthuis, D. Stein, C. Meyer, C. Dekker, Nano Lett. 6 (2006) 2232.
[15] X.C. Xuan, D.Q. Li, J. Power Sources 156 (2006) 677.
[16] Y. Ren, D. Stein, Nanotechnology 19 (2008) 195707.
[17] C. Davidson, X. Xuan, Electrophoresis 29 (2008) 1125.
[18] C. Davidson, X. Xuan, J. Power Sources 179 (2008) 297.
[19] R. Chein, H. Chen, C. Liao, J. Electroanal. Chem. 630 (2009) 1.
[20] R. Chein, C. Liao, H. Chen, J. Power Sources 187 (2009) 461.
[21] R. Chein, K. Tsai, L. Yeh, Electrophoresis 31 (2010) 535.
[22] C.-C. Chang, R.-J. Yang, Microfluidic. Nanofluidic. 9 (2010) 225.
[23] R. Chein, C. Liao, H. Chen, Nanoscale Microscale Thermophys. Eng. 14 (2010) 75.
[24] M. Wang, Q. Kang, Microfluidic. Nanofluidic. 9 (2010) 181.
[25] C.-C. Chang, R.-J. Yang, Appl. Phys. Lett. 99 (2011) 083102.
[26] D. Gillespie, Nano Lett. 12 (2012) 1410.
[27] J. Hoffmann, D. Gillespie, Langmuir 29 (2013) 1303.
[28] F.H.J. van der Heyden, D.J. Bonthuis, D. Stein, C. Meyer, C. Dekker, Nano Lett. 7 (2007) 1022.
[29] A.M. Duffin, R.J. Saykally, J. Phys. Chem. C 111 (2007) 12031.
[30] A.M. Duffin, R.J. Saykally, J. Phys. Chem. C 112 (2008) 17018.
[31] Y. Xie, X. Wang, J. Xue, K. Jin, L. Chen, Y. Wang, Appl. Phys. Lett. 93 (2008) 163116.
[32] A. Bentien, T. Okada, S. Kjelstrup, J. Phys. Chem. C 117 (2013) 1582.
[33] W.H. Koh, H.P. Silverman, J. Membr. Sci. 13 (1983) 279.
[34] P.N. Pintauro, R. Tandon, L. Chao, W. Xu, R. Evilia, J. Phys. Chem. 99 (1995) 12915.
[35] T.D. Gierke, G.E. Munn, F.C. Wilson, J. Polym. Sci. Part B Polym. Phys. 19 (1981) 1687.
[36] G. Gebel, J. Lambard, Macromolecules 30 (1997) 7914.
[37] H.G. Haubold, T. Vad, H. Jungbluth, P. Hiller, Electrochim. Acta 46 (2001) 1559.
[38] M. Litt, Ab. Pap. Am. Chem. Soc. 213 (1997) 33.
[39] M.H. Kim, C.J. Glinka, S.A. Grot, W.G. Grot, Macromolecules 39 (2006) 4775.
[40] K. Schmidt-Rohr, Q. Chen, Nature Mater. 7 (2008) 75.
[41] D.M. Rowe, Thermoelectrics Handbook: Macro to Nano, CRC, Boca Raton, FL, 2006.
[42] M.C. Ferrari, J. Catalano, M.G. Baschetti, M.G. De Angelis, G.C. Sarti, Macromolecules 45 (2012) 1901.
[43] T.A. Zawodzinski, C. Derouin, S. Radzinski, R.J. Sherman, V.T. Smith, T.E. Springer, S. Gottesfeld, J. Electrochem. Soc. 140 (1993) 1041.
[44] D.J.G. Ives, G.J. Janz, Reference Electrodes, Theory and Practice, Academic Press, New York, 1961.
[45] C.E. Evans, R.D. Noble, S. Nazeri-Thompson, B. Nazeri, C.A. Koval, J. Membr. Sci. 279 (2006) 521.
[46] A. Steck, H.L. Yeager, Anal. Chem. 52 (1980) 1215.
[47] T.D. Gierke, W.Y. Hsu, ACS Symp. Ser. 180 (1982) 283.
[48] I.A. Stenina, P. Sistat, A.I. Rebrov, G. Pourcelly, A.B. Yaroslavtsev, Desalination 170 (2004) 49.
[49] T. Okada, H. Satou, M. Okuno, M. Yuasa, J. Phys. Chem. B 106 (2002) 1267.
[50] T. Sata, Ion Exchange Membranes: Preparation, Characterization, Modification and Application, Royal Society of Chemistry, Cambridge, 2004.
[51] Malestrom, CRC Handbook of Chemistry and Physics, 2009.
[52] V.M. Barragan, C. Ruiz-Bauza, J.P.G. Villaluenga, B. Seoane, J. Colloid Interface Sci. 277 (2004) 176.
[53] J.P.G. Villaluenga, B. Seoane, V.M. Barragan, C. Ruiz-Bauza, J. Colloid Interface Sci. 268 (2003) 476.
[54] T. Okada, G. Xie, O. Gorseth, S. Kjelstrup, N. Nakamura, T. Arimura, Electrochim. Acta 43 (1998) 3741.
[55] T. Okada, S.K. Ratkje, H. Hanche-Olsen, J. Membr. Sci. 66 (1992) 179.
[56] G. Xie, T. Okada, Electrochim. Acta 41 (1996) 1569.
[57] V.M. Barragan, J.P.G. Villaluenga, M.R. Godino, M.A. Izquierdo-Gil, C. Ruiz-Bauza, B. Seoane, J. Power Sources 185 (2008) 822.
[58] M. Doyle, M.E. Lewittes, M.G. Roelofs, S.A. Perusich, R.E. Lowrey, J. Membr. Sci. 184 (2001) 257.
[59] L. Chaabane, G. Bulvestre, C. Larchet, V. Nikonenko, C. Deslouis, H. Takenouti, J. Membr. Sci. 323 (2008) 167.
[60] K.D. Sandbakk, A. Bentien, S. Kjelstrup, J. Membr. Sci. 434 (2013) 10.
[61] P. Sistat, G. Pourcelly, J. Membr. Sci. 123 (1997) 121.
[62] V.M. Barragan, C. Ruiz-Bauza, J. Colloid Interface Sci. 205 (1998) 365.
[63] G. Hoogers, Fuel Cell Technology Handbook, CRC Press, Boca Raton, Fla, 2003.
[64] P. Fievet, M. Sbai, A. Szymczyk, J. Membr. Sci. 264 (2005) 1.
[65] A.E. Yaroshchuk, Y.P. Boiko, A.L. Makovetskiy, Langmuir 18 (2002) 5154.